KERNFORSCHUNGSZENTRUM

KARLSRUHE

Mai 1965

KFK 302
SM 62/2

Institut für Neutronenphysik und Reaktortechnik
Institut für Angewandte Kernphysik

SUAK - A Fast Subcritical Facility for Pulsed Neutron Measurements

H. Borgwaldt, M. Küchle, F. Mitzel, E. Wattecamps

GESELLSCHAFT FUR KERNFORSCHUNG M.B.H.
KARLSRUHE

KERNFORSCHUNGSZENTRUM KARLSRUHE

May 1965

KFK 302

SM 62/2

Institut für Neutronenphysik und Reaktortechnik

Institut für Angewandte Kernphysik

SUAK - A Fast Subcritical Facility for Pulsed Neutron Measurements

H.Borgwaldt, M.Küchle, F.Mitzel, E.Wattecamps

Gesellschaft für Kernforschung m.b.H. Karlsruhe

INTERNATIONAL ATOMIC ENERGY AGENCY

SYMPOSIUM ON PULSED NEUTRON RESEARCH

May 10 - 14, 1965
Kernforschungszentrum Karlsruhe, Germany

SM 62/3

SUAK - A FAST SUBCRITICAL FACILITY FOR PULSED NEUTRON MEASUREMENTS +

H.Borgwaldt, M.Küchle, F.Mitzel, E.Wattecamps
Kernforschungszentrum Karlsruhe

1. Introduction

In the physics of thermal reactors a large amount of information has been obtained from the measurement of space and time eigenvalues of clean lattices. For fast systems with their very broad and system dependent energy spectrum the situation is much less favourable. Nevertheless, some exponential experiments have been performed. [1] But whereas in an exponential experiment a large amount of expensive material is wasted in the region where the spectrum reaches its asymptotic shape this is not the case in a pulsed neutron measurement. Therefore, the application of the pulsed source technique to fast systems seems to be attractive. However, since the asymptotic spectrum is only established via the multiplication process, a fairly high multiplication is required to get good time eigenvalues. If the amount of fuel available is limited, this can best be achieved with as little structural material as possible. For easier interpretation of the measurements an unreflected homogeneous system should be used. This leads to a small compact design with a relatively hard neutron spectrum.

+ The work was performed within the frame of the Fast Breeder Project-Association Karlsruhe-Euratom

Such an assembly has moreover the advantage of being very well suited for spectrum measurements by the time-of-flight technique since the short decay time allows very short flight paths to be used. This more than compensates the disadvantage of having only a small fraction of neutrons in the energy range where time-of-flight methods are applicable. Of course, the spectrum of such an assembly is quite different from that which is expected for a large dilute fast breeder. Nevertheless, calculational methods and cross section sets can be checked in that energy range where the Doppler effect is important and where no other techniques of spectrum measurements exist.

Therefore, in Karlsruhe in the framework of the fast breeder project, in addition to the large critical facility SNEAK and the coupled fast-thermal reactor STARK, the small flexible fast subcritical assembly SUAK has been constructed the fuel of which will later be used in the SNEAK assembly.

2. Description of the facility

The subcritical assembly consists of thin plates (2" x 2" x $\frac{1}{8}$") of 20% enriched uranium which are held in aluminium square tubes of 1 mm wall thickness. The tubes are closely packed together to form parallelepipeds of 27.0 cm, 32.3 cm, or 37.7 cm side length respectively. The height of the assembly is variable up to 35.1 cm by changing the filling height of the platelets. The tubes are closed at the top and at the bottom with 3 cm aluminium plugs and set with pins on an aluminium base plate of 3.0 cm thickness. To reduce backscattering of neutrons this assembly is located 5 m above the ground in the centre of a thin-walled building of dimensions 10 m x 15 m x 10 m. 3.5 m above the ground there is a grid on which the accelerator and auxiliary equipment is mounted. Fig.1 shows an artist's view of the assembly.

For radiation protection the building is surrounded at 25 m distance by a wall of 5.5 m height in which the control room is embedded. An evacuated flight tube of 50 cm diameter and variable length up to 22 m leads radially from the assembly to the wall. It is mounted on a bridge on which the heavily shielded detector can be moved on wheels to seal the end of the flight tube. An extension of the flight tube to 50 m is under construction.

The accelerator is a 200 kev Cockroft-Walton type generator constructed by W.Eyrich [2] that produces neutrons by the T(d,n)He^4 reaction. With a combined beam extraction and beam deflection pulsing device neutron bursts of 0.1 μsec width and triangular shape are produced at a repetition rate of up to $4 \cdot 10^4$ cycles per second.

When building up the assembly the approach to criticality was controlled by a multiplication measurement. For that purpose a Po-Be-source was inserted at the bottom of the central fuel element and the neutron flux as a function of the number of fuel elements was measured with 3 long counters placed on different sides of the assembly at a distance of about 1 m. Two of the central elements acted as safety rods. They were not plugged at the base plate but movable by control rod drives from below. At a preset flux level they would drop out of the assembly, thus reducing the multiplication.

Since it was not allowed to go to a higher multiplication than corresponds to $k_{eff} = 0.90$ a fairly accurate determination of k_{eff} during the build up of the assembly was necessary. Therefore, the expected counting rate as a function of the number of fuel elements N was calculated using several hundred spatial harmonic modes. In view of the small number of elements and the odd shape of the configurations during build up of the assembly, from each counting rate a value was subtracted that was obtained from the same configuration but with the elements filled with lead. This greatly reduced shadowing and scattering effects from single elements. When plotting this corrected inverse multiplication $^1/M$ vs. $^1/\sqrt{N}$ an approximately straight line was found for $M > 5$ which could be extrapolated to give the critical mass. Adjusting the calculation to this value the k_{eff} of the assembly was found. In practice the agreement between the experimental and theoretical critical number of fuel elements was so good that only an adjustment of 0.5% in k_{eff} was required.

3. The theory underlying the pulsed neutron measurements

In view of the small size and the simple shape of the SUAK assemblies the decay of the neutron field after injection of a neutron burst was treated in a space independent multigroup diffusion approximation. Leakage was taken into account by introduction of a buckling B^2 that was calculated from the geometrical dimensions with an extrapolation length of $d = 0.71\ \bar{\lambda}_{tr}$ where [3]

$$\bar{\lambda}_{tr} = \sum_{i=1}^{G} \phi_i \phi_i^{*} \lambda_{tr\,i}^2 \Big/ \sum_{i=1}^{G} \phi_i \phi_i^{*} \lambda_{tr\,i} \quad . \tag{1}$$

ϕ_i and ϕ_i^{*} are the static flux and importance spectra and G is the number of groups.

The top and bottom plug and the base plate were taken into account by calculating the savings with a one dimensional multigroup diffusion code. [4] This approximation was checked by measuring the reactivity effect of an additional aluminium plate of 3 cm thickness placed at one side of the assembly. The measured and calculated values agreed well within the limits of error. The error introduced from the diffusion approximation was checked by comparing a static S_4 calculation with a diffusion calculation. The S_4 calculation gave a k_{eff} which was about 2% higher.

The multigroup constants used were based on the Karlsruhe version of the 16-group cross section set of Yiftah, Okrent, and Moldauer [5] (YOM) and on the 26-group data of Abagjan, Bazazjanc, Bondarenko, and Nikolaev [6] which include corrections for resonance self shielding, in the following called ABN.

Three types of solutions of the multigroup diffusion equation have been used. In view of the short prompt neutron decay times and high repetition rates of pulsing the delayed neutrons were always treated as a constant background.

a) Determination of decay constants

The multigroup equations were Laplace transformed and written in a form that helps to find the time eigenvalues

$$\frac{1}{k(p,B^2)} \left[\sum_{j=1}^{G} (\nu\sigma_f)_j \; \phi_j(p) \right] \chi_i + \sum_{j=i+1}^{G} \sigma_s(i,j)\, \phi_j(p) - \left(\sigma_{rem,i} + D_i B^2 + \frac{p}{v_i}\right) \phi_i(p) = 0 \qquad (2)$$

with the normalization of ϕ_j:

$$k(p,B^2) = \sum_{j=1}^{G} (\nu\sigma_f)_j \; \phi_j(p) \; .$$

Here p is the Laplace parameter, the ϕ_j are the transformed group fluxes, ν is the average number of prompt fission neutrons and $\sigma_s(i,j)$, $\sigma_{rem,i}$, and $\sigma_{f\,i}$ are the macroscopic group transfer, removal, and fission cross sections, respectively. χ_i is the fraction of the fission spectrum in the i-th group, D_i is the diffusion coefficient, and k(p) is the Laplace transform of the first generation multiplication kernel which is an obvious generalization of k_{eff} of the stationary reactor theory. [1] Eigenvalues of eq.(2) are the p-values for which $k(p_n) = 1$; $n = 1, 2 \ldots G$. [7] The smallest eigenvalue should be the fundamental mode decay constant.

But for fast systems with a low multiplication ($k_{eff} < 0.90$) it happens that whereas the bulk of neutrons are decaying exponentially with a time constant

$$\alpha \approx \frac{1 - k_{eff}(1 - \beta)}{l}$$

there is a small fraction of low energy neutrons not participating in this time behaviour but decaying more slowly and in a non-exponential way. These had to be described by continuous eigenvalues.

In the multigroup calculations the existence of these neutrons is reflected in the fact that the decay constant of the bulk of neutrons we are looking for is not necessarily the lowest eigenvalue but is followed by others. However, if the multiplication is not too low, the interesting mode can easily be found since it is the first eigenvalue p_n coming from positive p-values which is clearly distinguished from any pole of k(p). [7] This phenomenon is illustrated in Fig.2.

b) Calculation of the complete time behaviour of the neutron decay

When the multiplication is too low ($k_{eff} < 0.80$) the first part of the decay of the neutron field after a pulse is strongly influenced by energy harmonics whereas the last part is governed by the low energy neutrons mentioned above. Therefore, no decay constant can be extracted from the measured time behaviour. To be able to interpret measurements even in that case the complete time behaviour of the neutron field after a pulse has been calculated.

---

1) $\frac{1}{k(p)}$ can be described as the factor by which ν had to be multiplied to make p and B^2 exist in the reactor at the same time.

For that reason a Fourier series expansion of the time dependence of the neutron flux with a rectangular source distribution has been performed

$$\phi(t) = \sum_{n=1}^{\infty} \phi_n \, e^{i\omega_n t} \quad . \qquad (3)$$

The Fourier coefficients were calculated from the multigroup diffusion equations with that source. Up to a hundred frequencies have been included. Moreover, the energy distribution of the source and the energy sensitivity of the detector could be taken into account.

Calculations with the 16-group YOM-set and with the 26-group ABN-set which extend down to the thermal region showed a fairly good exponential decay for $k_{eff} > 0.70$.

c) Correlation between decay constant, reactivity, and neutron lifetime

In the interpretation of pulsed neutron measurements the relation

$$\alpha = \frac{1 - k_{eff}\,(1 - \beta)}{l} \qquad (4)$$

is often used, where α is the prompt neutron decay constant and l is the neutron lifetime. To check the validity of this equation a power series expansion of $\frac{1}{k(p)}$ in the vicinity of $p = 0$ was made

$$\frac{1}{k(p)} = \frac{1}{k(0)} \left[1 + l_1 p + l_2 p^2 + l_3 p^3 + \dots \right]$$

where $k(0) = k_{eff}(B^2)\,(1-\beta_{eff})$ and l_1 is the neutron lifetime. The correction terms to eq.(4) l_2 and l_3 were computed from a third order perturbation theory. For $k_{eff} = 0.87$ the correction amounts to about 10% in α.

4. Measurements of the neutron decay

From the calculations of the time decay of the neutron field it turned out that a good exponential could only be expected for $k_{eff} > 0.7$. On the other hand, for safety reasons the systems were restricted at present to $k_{eff} < 0.90$. Since moreover the amount of fuel available was limited to 120 kg U^{235} in the form of 20% enriched uranium no large variation in size and composition was possible but the system with the highest multiplication was built up.

This was a block consisting of 6 x 6 elements filled up to the top with 20% enriched uranium only. Any additional material would have reduced the multiplication or would have softened the neutron spectrum too much. The parameters of the assembly are given in Table I.

The assemblage was interrupted at 5 x 5 elements to perform check measurements. These data are also given in Table I. Since the decay times of these systems were in the range of 100 nsec to 200 nsec a timing accuracy of about 10 nsec was required. This was achieved with a Stilbene scintillator used for proton recoil measurements and fission counters operating with cross-over-pick-off gates. The Stilbene crystal was fixed between two multipliers. A slow coincidence from the two was used for noise suppression; pulse shape discrimination as proposed by Owen [8] gave a signal free of γ-background from one multiplier and a triple coincidence of these signals opened a gate for the fast signal taken from the anode of the other multiplier.

A TMC 256-channel time analyser with the model 219 plug-in unit was used, capable of channel width down to 10 nsec. The target current pulse triggered the analyser.

For the measurements with the 25 element assembly the target was outside and one element was withdrawn to insert a U^{235}-fission counter in a position where the most important spatial harmonics were suppressed.

The measured time dependence of the neutron intensity after subtraction of the constant delayed neutron background is given in Fig.3. When the transients have died away there is a small interval where the time behaviour looks exponential but then it is followed by an slower decaying tail of much higher intensity than predicted by the calculation which is also included in the Figure. The calculation was performed for the unperturbed case with the ABN cross section set. [6] Measurements with the unperturbed assembly and the proton recoil detector outside showed a time behaviour that differed mainly in the transients.

The 36 element assembly measurements have been made with fission counters [2)] coated with Np^{237}, U^{238}, and U^{235}, located inside and outside the

---

2) 20^{th} Century Electronics type FC 165

assembly. When inserted in the assembly the counters were completely embedded in the fuel so that the perturbation now was relatively small. A good exponential decay was always observed. Due to energy harmonics there was a small difference in the transients between the Np^{237} and the U^{235} fission counter measurements and a larger difference between the U^{235} and the U^{238} results for the time interval from the beginning up to 400 nsec. The time decay as measured with a Np^{237} fission counter outside the assembly is included in Fig.3. No calculated curve is given but the decay times are compared in Table I.

The experimental decay time is about 15% longer than predicted by the calculation based on the ABN-cross sections and 30% longer than calculated from the YOM-data. Since the agreement in $1 - k_{eff}$ is much better this seems mainly to be due to errors in the calculation of the neutron lifetime. A calculation with the ABN-set without correction for resonance self-shielding showed that there is practically no self-shielding in the SUAK-assemblies. Therefore, the difference in the lifetimes as calculated from the YOM-and from the ABN-data must be due to differences in the cross sections.

The values in the table are taken from eigenvalue calculations, but practically the same values were found from a plot of the time dependent neutron flux.

To check the influence of backscattered neutrons a measurement with the assembly covered with cadmium was made. No difference in the neutron decay apart from the reflector effect of cadmium was observed.

An additional check was the determination of reactivity from the ratio of the time-averaged prompt and delayed neutron fluxes as proposed by Gozani [9]

$$\frac{\bar{\phi}_{prompt}}{\bar{\phi}_{delayed}} = - \frac{\rho}{\beta_{eff}} .$$

Since the prompt neutron decay time is short and the repetition rate is high, room return neutrons would give an almost constant background. This adds to the delayed neutron flux and leads to a wrong experimental flux ratio. This is particulary serious for systems which are subcritical to this extent.

For the determination of the fundamental mode prompt neutron flux the finite width of the source burst had to be taken into account. Though the almost triangular shape of the source burst has been measured, some uncertainty is due to this correction. β_{eff} was determined from the measured fractions of U^{238} and U^{235} fissions of the assembly. The minor importance of the delayed neutrons was taken into account. As an average from different measurements with the fission counter inside and outside of the assembly

$$k_{eff} = 0.88 \pm 0.02$$

was obtained.

An evaluation with the method as proposed by Garelis gave well within the limits of error the same result. [10]

The fact that the value is higher than the result of the stationary measurement could be explained in the way that (17 ± 5) % of the constant background is due to room scattered neutrons. However, in view of the uncertainties from the finite pulse width correction, from the determination of β_{eff}, and from a possible presence of delayed neutron harmonics, the conclusion is not very stringent.

In addition to the measurements with the unperturbed assembly, the reactivity effects of an aluminium plate and of the withdrawal of single elements have been determined by the pulsed source method.

5. Measurements of neutron spectra by the time-of-flight technique

If the build-up and decay of the neutron field in an assembly after a neutron burst injection is short compared with the flight-time of the neutrons from the assembly to the detector, what is measured is essentially the stationary spectrum of the subcritical assembly with a continuously running source. This, of course, differs from the spectrum of the critical assembly and from the asymptotic spectra in time or in space. But if it is just this spectrum which we calculate, no fundamental problems of interpretation of the measured spectra arise. The spectrum is highly space dependent, however, and so far measurements from two positions have been made:

1. The spectrum from the centre of the assembly. Here, no flux gradient difficulties appear if the target position is also at the centre of the assembly.

2. The leakage spectrum from the surface. Here, no beam extraction problems arise.

In both cases, however, the problems of neutron collimation and determination of the background have to be solved first. Since the measurements started very recently, the investigations so far have concentrated mainly on these points.

A large-area neutron detector of high sensitivity in the kev-region but with moderate time resolution properties is required. Therefore, a Li^6-loaded glass scintillator of 4 $^3/16''$ diameter and 1'' thickness was chosen. This detector is very sensitive to kev-neutrons, but it is also black to slow neutrons and sensitive to γ-rays. This is particulary serious since the assembly is completely unshielded. Therefore, the scintillator is surrounded by a heavy shield consisting of concentric annular cylinders of 4 mm B^{10}-powder, 5 cm lead and 40 cm of a mixture of paraffin and Li_2CO_3 which has an overall length of 170 cm. The whole shield is placed on a trolly. The flight tube is of variable length ranging from 5 m to 22 m. It is evacuated and sealed on both sides by 2 mm and 1.5 mm aluminium windows, respectively. In the flight tube steel collimators of 20 cm thickness were placed at $^1/4$, $^2/4$, and $^3/4$ of the flight path. Their inner part consisted of replaceable annular cylinders of CUNIFER 30 to adjust the opening of the collimator to the requirements of the experiments. The outer diameter of 41 cm was chosen to prevent primary source neutrons from hitting the shield.

To measure the spectrum from the centre of the assembly a difference technique was applied which allows the most reliable background determination. For these measurements, the central row of fuel elements was replaced by a horizontally stacked row which left the dimensions of the assembly unchanged. The fuel of the central element of this row could be removed to generate a horizontal through-channel of 5 cm x 5 cm. This channel could be loaded half from the side opposite to the detector.

For spectrum measurements from the centre all collimators but the first one had an inner diameter of 12.5 cm. The latter selects a circular area of 35 cm^2 centred at the beam hole axis, that means 25 cm^2 from the central region and 10 cm^2 from the surface.

The spectrum from the central region of the assembly is obtained by subtracting the time-of-flight distribution with the through-channel from the time-of-flight distribution obtained with the channel loaded with fuel up to the centre. It has not been investigated whether the spectrum in the beam differs from the spectrum in the centre of the assembly. Wall-scattering effects at the extraction channel were certainly reduced by the difference method.

Since the withdrawal of the fuel plug from the central channel reduces the multiplication of the assembly by $\Delta k_{eff} = 0.014$ it also reduces the background. Therefore, the measurements were normalized to the same counting rate of a long counter.

For the measurements of the leakage spectrum from the surface of the assembly, all collimators had an inner diameter of 12.5 cm which selected a circular area of 123 cm^2 at the centre of one side of the assembly. Much attention has been given to the determination of the background. In order to gain a better understanding of the methods used, different sources of background have to be distinguished, the most important ones being:

1. Permanent background due to
   a) radioactive impurities contained in the Li^6-glass scintillator,
   b) cosmic radiation,
   c) photomultiplier noise.
2. Time-independent background from the accelerator due to
   a) delayed neutrons,
   b) prompt neutrons slowed down in the shield.
3. Time-dependent background due to
   a) air, wall, and ground-scattered neutrons,
   b) beam neutrons scattered in the detector shield which, therefore, are detected at a time later than corresponds to their flight-time,
   c) neutrons scattered at the inner collimator walls,
   d) neutrons penetrating the collimator,
   e) prompt γ-rays from fission and inelastic scattering,
   f) neutrons and γ-rays from the accelerator produced outside the assembly and not shadowed by the collimator.

The permanent background has been measured when the accelerator was switched off. Its contribution was respectively 0.2%, 1.8%, and 12% at neutron energies of 300 kev, 100 kev, and 10 kev.

The time independent background was measured in the time channels preceding the accelerator burst. It amounts to 0.8%, 5%, and 32% of the signal at neutron energies of 300 kev, 100 kev, and 35 kev, respectively. To measure the time-dependent background different methods have been investigated:

1. To determine the γ-background time-dependent pulse height spectra of the Li^6-detector have been measured with a time resolution of 500 nsec. From each spectrum the γ-ray contribution has been obtained by proper extrapolation of the pulse height spectrum from the region where no neutrons can occur into the region used for neutron detection.

2. Furthermore, the γ-ray background has been determined with a Li^7-detector which is insensitive to neutrons, but equally sensitive to γ-rays as the Li^6-detector.

3. Shadowing the detector by 20 cm Cunifer 30 practically suppresses the neutron beam and allows to determine background type 3a and f. An additional plate of 10 cm plastic placed at the back of the first collimator should transform background type 3d to an almost time-independent background. A measurement with such a plate showed that the effect was very small.

4. The background type 3b and c is the most difficult to measure. Here, a plug is required which is transparent to all neutrons, except for the neutrons in the energy range to be measured. For these it should be completely black. This can be approximated for selected energies by a material with black resonances. Since the cross section peaks at the different resonances are of different height the thickness of the transmission probe has to be optimized for each energy.

5. Furthermore, in the energy region between resonances it is possible to determine the background from extrapolation of the transmission of probes of different thickness to zero transmission using the known total cross section.

So far, measurements have been made with a flight path of 11.5 m at assembly No.2. The target was located at the centre of the assembly. The build-up and decay of the neutron field after the neutron burst had a half width of 300 nsec. The repetition frequency of the accelerator was $25 \cdot 10^3$ cycles per second and the intensity was 10^4 neutrons per burst. A TMC 256 channel analyser with a model 201 plug-in unit was set at a channel width of 125 nsec.

Other data of the measurements are listed in Table II. The background measurements for the leakage spectrum are illustrated in Fig.4. The close agreement between the results from the shadow-cone and from the black resonance measurements indicates that the background type 3b and c is rather small.

The time-of-flight distributions have been corrected for background, for the transmission of the aluminium windows, and for the energy dependence of the Li^6-detector. The detector has previously been calibrated in the energy range from 5 kev to 320 kev with monoenergetic neutrons from a van de Graaff generator. The measured sensitivity curve corresponds to the expected efficiency as deduced from the $Li^6(n,\alpha)$-cross section.

No resolution correction has been applied so far. Since the main purpose of the measurements is to check calculations, this correction could be avoided at all when measured and calculated time-of-flight distributions were compared.

In Fig.5 the measured parts of the spectra are given together with the calculated flux shapes. The measurements are normalized so as to agree with the calculation at about 100 kev. The one-dimensional 16-group diffusion calculation based on the YOM-data serves only as a rough indication of the SUAK spectra. For comparisons with the measurements, more sophisticated calculations will later be used. The measured spectra are much softer than the calculated ones. No conclusion should be drawn, however, unless the measurements were extended to lower as well as to higher energies. Here, it seems possible to go up to more than 1 Mev. If the length of the flight path and the channel width were optimized, the counting rate per channel Z is given by

$$Z(t) = \text{const.}\,\eta(E)\,\emptyset(E)\,\alpha^2\left(\frac{\Delta E}{E}\right)^4$$

where η is the sensitivity of the detector, $\emptyset(E)$ is the neutron spectrum, and α is the prompt neutron decay constant. Since $\emptyset$ is increasing, where η is decreasing, similar counting rates at the same resolution can be expected for higher energies as have been obtained so far. The approximate resolutions obtainable at various energies for the flight paths s foreseen are given in the following Table.

$\frac{\Delta E}{E}$	s = 5.5 m	11.5 m	21.5 m	50 m
5%	4.5 kev	18 kev	76 kev	390 kev
10%	18 kev	86 kev	300 kev	1.5 Mev

Acknowledgement

The authors would like to acknowledge the great help they have had from D.Schreier throughout the work, they further are indebted to W.Eyrich for setting up and servicing the accelerator. Thanks are also due to K.H.Beckurts for many suggestions and stimulating discussions.

References

[1] SNELL, A.H., CF-589 (1943);
MARTENS, F.H., ANL-5379 (1955);
CHEZEN, C.G., Nucl. Sci. and Eng. 8 (1960) 652;
BEETS, C., CAMPAN, J.L., DECKERS, H., ZALESKI, C.P., React. Sci. and Techn. 16 (1962) 221;
BONDARENKO, I.I., GOLUBOV, V.I., ZUONAREV, A.V., NIKOLAEV, M.N., ORLOV, M.J., UZNADZE, O.P., Atom. Energ. 17 (1964) 113.

[2] EYRICH, W., Nukleonik 4 (1962) 167.

[3] BORGWALDT, H., Nukleonik 5 (1963) 27.

[4] MÜNZNER, W., Internal Karlsruhe Report INR-103 (1964).

[5] YIFTAH, S., OKRENT, D., MOLDAUER, P.A., Fast Reactor Cross Sections, Pergamon Press (1960).

[6] ABAGJAN, L.P., BAZAZJANC, N.D., BONDARENKO, I.I., NIKOLAEV, M.N., INDSWG-17 (1963).

[7] STORRER, F. and STIEVENART, M., EUR 593e (1964).

[8] OWEN, R.B., Nucleonics 17 (1959) 92.

[9] GOZANI, T., Nukleonik 4 (1962) 348.

[10] GARELIS, E. and RUSSEL, J.L., Nucl.Sci. and Eng. 16 (1963) 263.

List of Tables and Figures

Table I

Measurement of neutron decay

Atomic densities of the assemblies		$N\text{-}U^{235} = 0.821 \cdot 10^{22}/cm^3$ $N\text{-}U^{238} = 3.284 \cdot 10^{22}/cm^3$ $N\text{-}Al^{27} = 0.437 \cdot 10^{22}/cm^3$
Experimental critical mass corrected for savings		248 ± 10 kg U^{235}
Assembly number	1	2
Number of elements	25	36
Loading $[kg\ U^{235}]$	82.24 kg	118.5 kg
Size including savings	26.9 x 26.9 x 38.3 $[cm^3]$	32.3 x 32.3 x 38.3 $[cm^3]$
Geometric buckling B^2	$2.431 \cdot 10^{-2} [cm^{-2}]$	$1.877 \cdot 10^{-2} [cm^{-2}]$
k_{eff} from $^1/M$-measurements	≈ 0.75	0.86 ± 0.01
k_{eff} from pulsed measurements (area method)	-	0.88 ± 0.02
k_{eff} calculated from ABN-set	0.765	0.864
k_{eff} calculated from YOM-set	0.754	0.843
$(\frac{1}{\alpha})$ measured	no exponential decay	230 ± 3 nsec
$(\frac{1}{\alpha})$ calc. ABN	122 nsec	205 nsec
$(\frac{1}{\alpha})$ calc. YOM	108 nsec	176 nsec

Table II

Spectrum measurements

Type of measurement	neutron energy	energy resolution	signal / background	statistical error	running time [hours]
leakage spectrum from the surface	88 kev 35 kev	10% 6.5%	5.0 1.32	1% 2.5%	8 h
beam spectrum from the centre	88 kev 35 kev	10% 6.5%	0.74 0.36	2.2% 6.1%	40 h

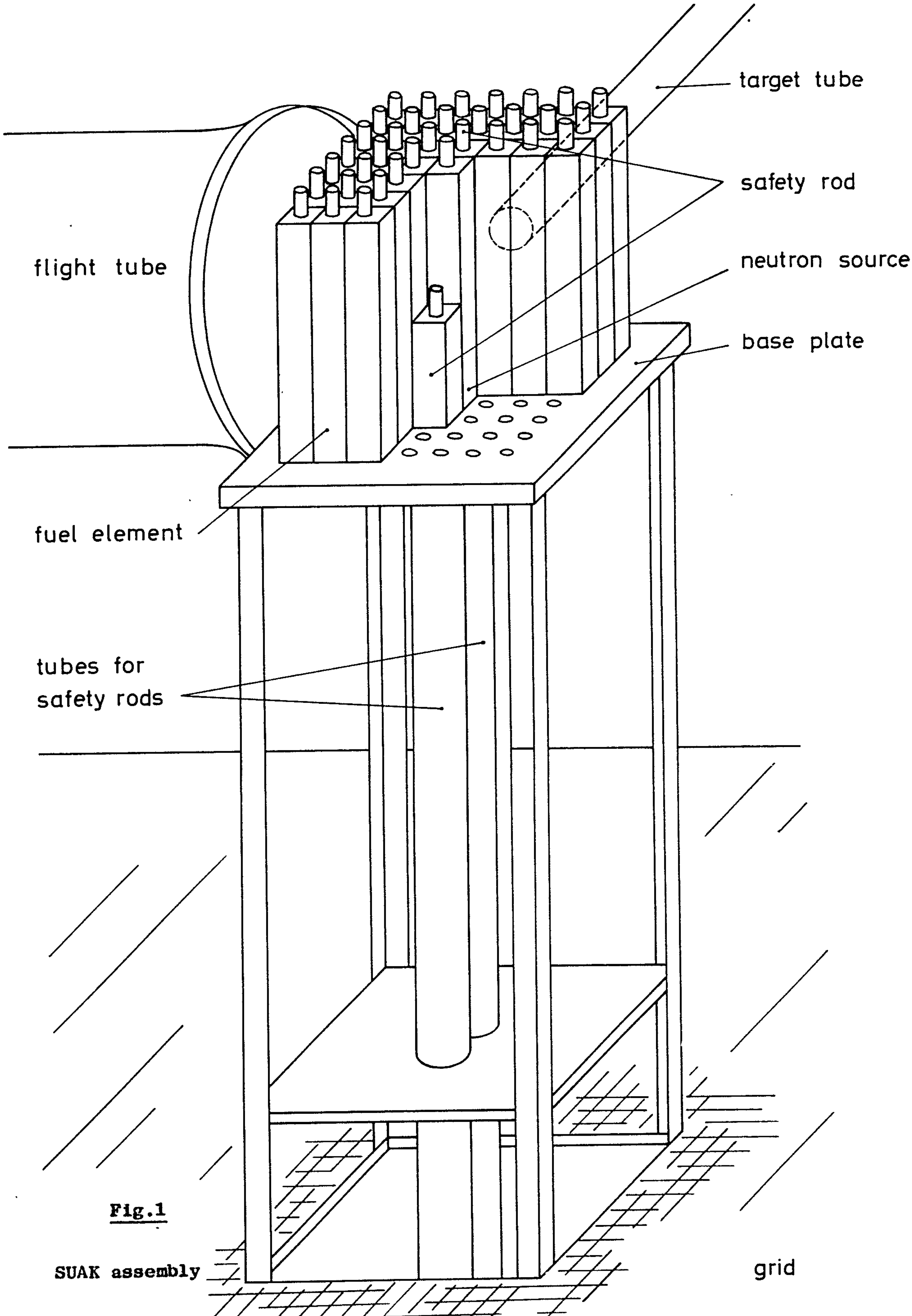

Fig.1

SUAK assembly

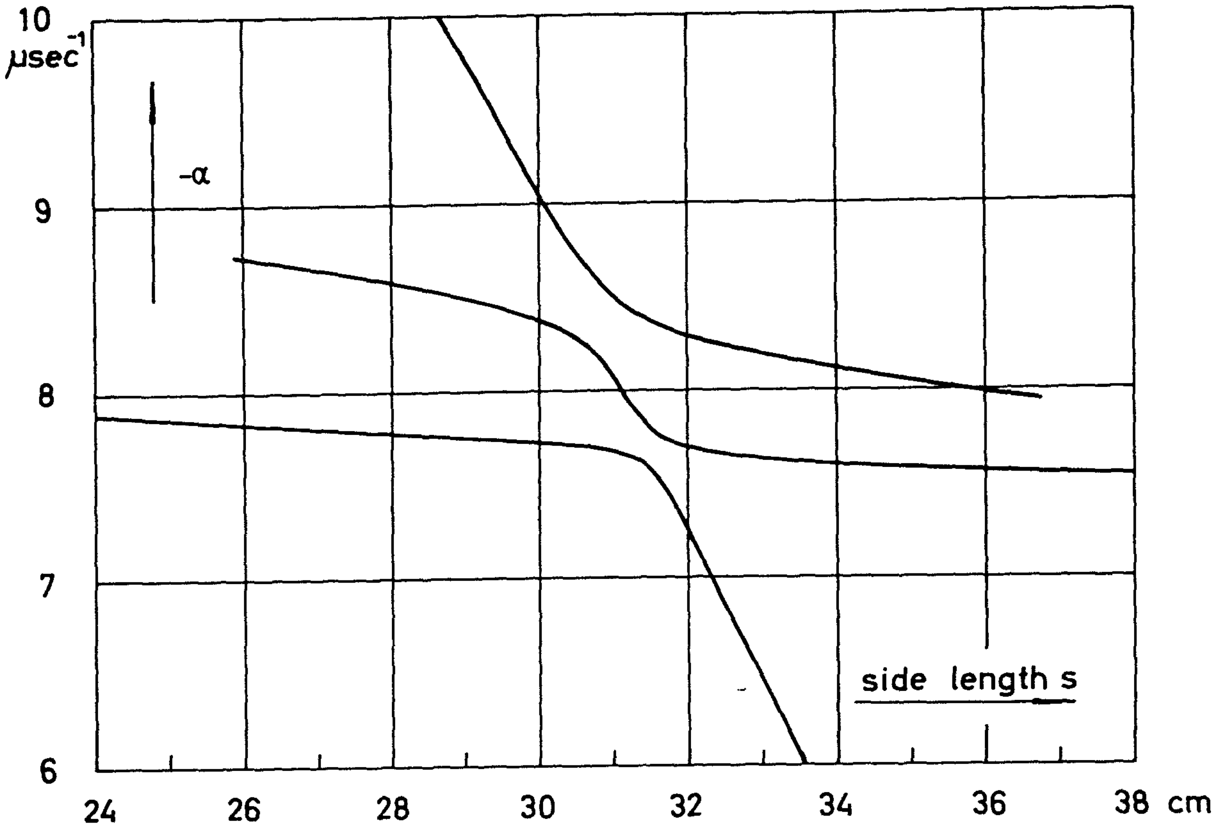

Fig.2

The prompt neutron decay constant as calculated from the 16-group YOM-set versus the sidelength s of a cube consisting of 20% enriched uranium. The usual continuous shape is interrupted, and it is the fundamental mode only for $s > 32$ cm. For 31 cm $< s <$ 32 cm it is the first harmonic, for $s < 31$ cm it is the second harmonic and so on.

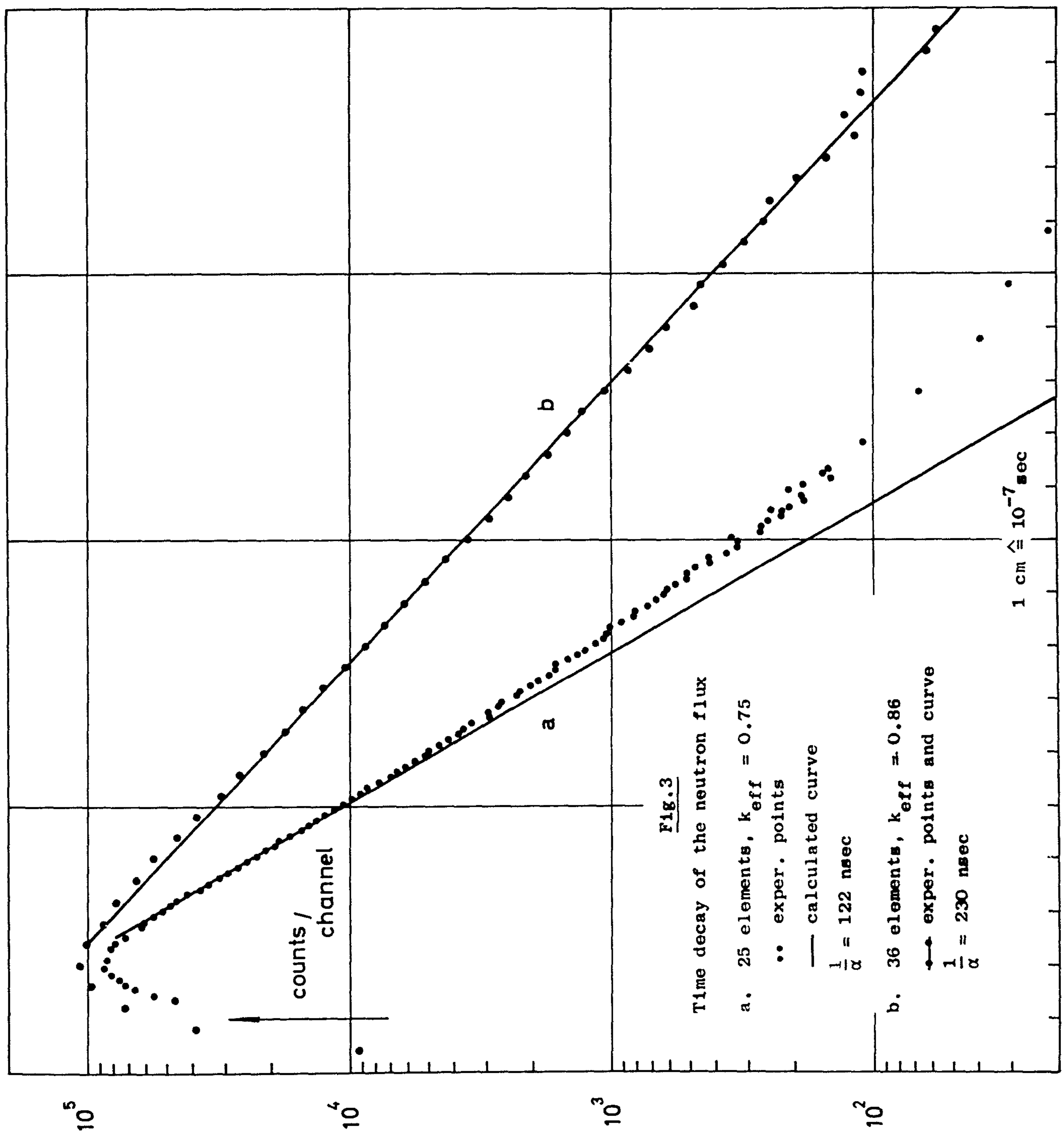

Fig.3

Time decay of the neutron flux

a. 25 elements, k_{eff} = 0.75

•• exper. points

— calculated curve

$\frac{1}{\alpha}$ = 122 nsec

b. 36 elements, k_{eff} = 0.86

•—• exper. points and curve

$\frac{1}{\alpha}$ = 230 nsec

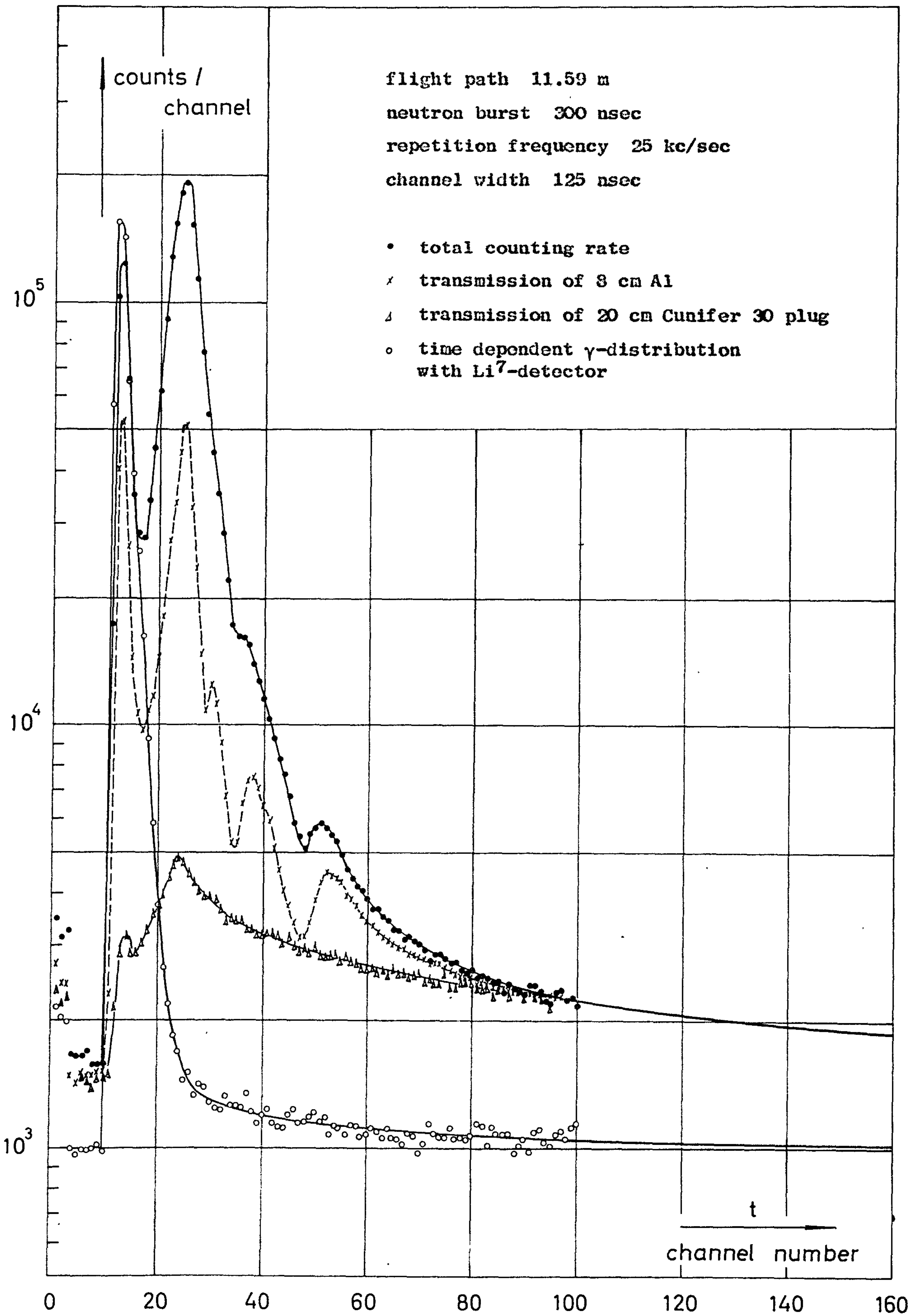

Fig.4

Time-of-flight distributions for leakage spectrum

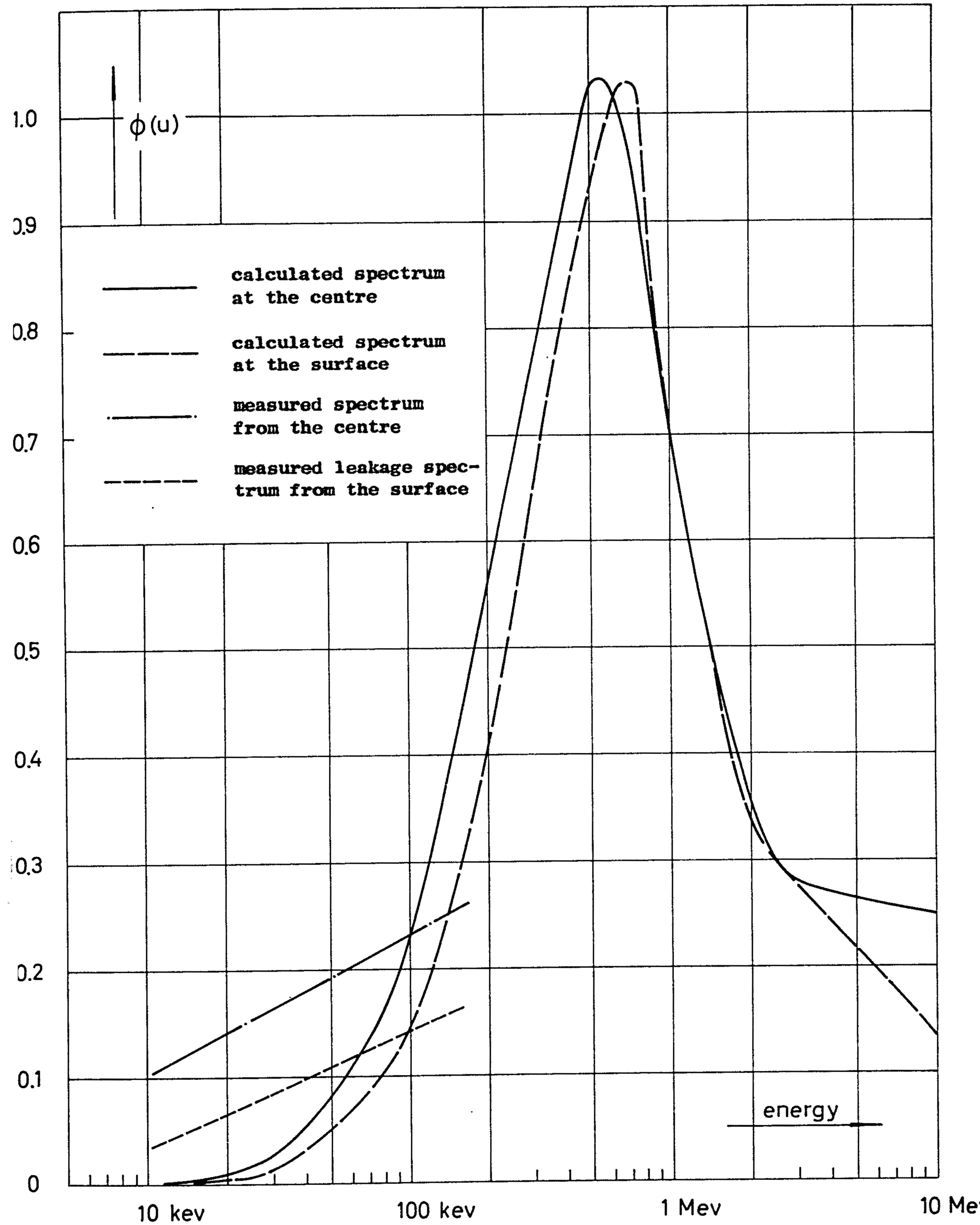

Fig.5

Spectra of the SUAK assembly